J Fluoresc (2013) 23:767–776
DOI 10.1007/s10895-013-1182-1

ORIGINAL PAPER

Bis-Benzimidazolyl Diamide Based Fluorescent Probe for Copper(II): Synthesis, Structural and Fluorescence Studies

Kuldeep Mahiya · Pavan Mathur

Received: 1 October 2012 / Accepted: 24 February 2013 / Published online: 15 March 2013

Abstract A new fluorescent probe based on a *bis*-benzimidazole diamide N^2,$N^{2'}$-*bis*[(1-ethyl-benzimidazol-2-yl)methyl] biphenyl-2,2′-dicarboxamide ligand $\mathbf{L_1}$ with a biphenyl spacer group and a Copper(II) trinuclear metallacycle has been synthesized and characterized by X-ray single crystallography, elemental and spectral (FT-IR, ^{1}H & ^{13}C NMR, UV-Visible) analysis. The fluorescence spectra of $\mathbf{L_1}$ in MeOH show an emission band centered at 300 nm. This band arises due to benzimidazolyl moiety in the ligating system. The diamide $\mathbf{L_1}$ in the presence of Cu^{2+} show the simultaneous 'quenching' of (300 nm) and 'enhancement' of (375 nm) emission band. Similar fluorescence behavior was found in water–methanol mixture (9:1). The new emission band at 375 nm is attributed to intra ligand π–π* transition of the biphenyl moiety. $\mathbf{L_1}$ exhibited high selectivity and sensitivity towards Cu^{2+} in both the medium over other common metal ions like Ni^{2+}, Co^{2+}, Mn^{2+}, Mg^{2+}, Zn^{2+}, Pb^{2+} and Hg^{2+}. The binding constant with Cu^{2+} was calculated by the Benesi-Hildebrand equation. Selective "off-on-off" behavior of $\mathbf{L_1}$ in methanol has also been studied. The fluorescent intensity of 375 nm bands in $\mathbf{L_1}$ enhances (turns-on) upon addition of Cu^{2+} and quenches (turn-off) upon addition of Na_2-EDTA.

Keywords *bis*-benzimidazole diamide · Biphenyl · Fluorescence · Crystal structure · Copper(II)

Electronic supplementary material The online version of this article (doi:10.1007/s10895-013-1182-1) contains supplementary material, which is available to authorized users.

K. Mahiya · P. Mathur (✉)
Department of Chemistry, University of Delhi,
Delhi 110007, India
e-mail: pavanmat@yahoo.co.in

Introduction

Transition metal ions can be detected in low concentration by fluorescence spectroscopy and it is therefore of great importance in areas of human health and environment [1–3]. A large numbers of new fluorescent probes that detect transition metal ions in solution have been reported [4–15]. A new area where organic molecules are utilized to act as sensors, switches, triggers and logic gates has developed rapidly. Some of these systems utilize a fluorescent signal due to photoinduced electron transfer (PET) mechanism to understand a molecular recognition event [16]. Further a number of fluorescent probes exhibiting the turn "off-on-off" switch involving photoinduced electron transfer (PET) phenomenon for protons and metal ions [17–24], intramolecular charge transfer (ICT) process [25], Chelation Enhanced Fluorescence [26, 27] have also been reported.

Copper plays an important role in various biological processes [28–30]. The limit of copper in drinking water has been set to 1.3 ppm (20 μM). Since, exposure to a high level of copper even for a short period of time can cause gastrointestinal disturbance and long-term exposure can cause liver or kidney damage [31, 32]. Thus detection of copper(II) from various sources including those in waste water outlets, electroplating waste and other metal processing industries is important. Peptides structures have been reported that show selective binding towards Cu^{2+} [33–35]. Owing to its high detection sensitivity and operational simplicity fluorescent sensor of Cu^{2+} is used to elucidate the role of metal ion in vivo as well as to monitor its concentration in metal-contaminated sources. In recent years, many fluorescent chemosensors have been reported which detect Cu^{2+} in organic and aqueous-organic media in the range from 5 μM–20 μM [11, 14, 36, 37]. The present system detects 12.5 μM of Cu^{2+} in organic and organic-aqueous media.

In the present study, we describe the synthesis and characterization of a new fluorescent benzimidazolyl diamide ligand $\mathbf{L_1}$ having a biphenyl spacer. The ligand detects Cu^{2+} in presence of metal ions like Ni^{2+}, Co^{2+}, Mn^{2+}, Mg^{2+}, Zn^{2+}, Pb^{2+} and Hg^{2+}. While with Cu^{2+} and Na_2-EDTA, a turn "off-on-off" signaling behavior is observed for the fluorescent benzimidazolyl diamide ligand. To the best of our information, *bis*-benzimidazolyldiamide fluorescent probes having a biphenyl spacer exhibiting the turn "off-on-off" behavior have not yet been reported [38].

Experimental Section

Materials and Instruments

All the reagents and solvents were purchased from commercial sources. 2,2′-Diphenic acid was purchased from Sigma-Aldrich and all other chemicals were of analytical grade and used as received. 2-Aminomethylbenzimidazolyl dihydrochloride was prepared following the procedure reported by Cescon and Day [39]. HPLC grade solvents and double distilled water was used for spectral work. IR spectra were obtained in the solid state as KBr pellets on a Perkin Elmer FTIR- 2000 spectrometer. Electronic spectra were obtained on a Shimadzu UV-vis-1601 Spectrometer. The micro analytical data were obtained from the Elemental Analyzer System GmbH Vario EL-III instrument. ^{1}H (400 MHz) and ^{13}C (125 MHz) NMR spectra were recorded on a JEOL ECX-400P NMR spectrometer using tetramethylsilane (TMS) as an internal reference. Fluorescence spectra were recorded in methanol as solvent on a Varian CARY Eclipse fluorescence spectrophotometer. The single crystal diffraction data were collected on an X'Calibur single crystal X-ray diffractor having CCD camera [Mo/Kα radiation (λ=0.71073 Å)] at Department of chemistry, University of Delhi, India.

Fluorescence Measurements

The stock solution of $\mathbf{L_1}$ (5000 μM) for electronic absorption and emission spectral studies was prepared using HPLC grade methanol. The solutions of all metal ions were prepared by dissolving nitrate salts in HPLC grade methanol and double distilled water (5000 μM). In the titration studies typically, 2.0 ml solution of $\mathbf{L_1}$ (100 μM) was taken in a quartz cell of 1 cm path length and 12.5 μM of metal ions were added gradually to the solution. The resulting solution was mixed thoroughly and immediately a fluorescence spectrum was recorded. For fluorescence intensity measurements, the excitation and emission wavelengths were fixed at 277 nm and 285 nm, respectively. The slit widths were 5 nm/5 nm.

Synthesis of the Diamide Ligands

Synthesis of N^2,$N^{2'}$-bis[(1H-benzimidazol-2-yl)methyl] biphenyl-2,2'-dicarboxamide (A)

This compound was prepared by following the literature procedure as reported by Mahiya and Mathur [40] and Vagg et al. [41] and outlined in Scheme 1. A solution of 2,2′-Diphenic acid (8.25 mmol, 2.0 g) & 2-Aminomethylbenimidazolyl dihydrochloride (16.51 mmol 3.63 g) in 25 ml of pyridine was stirred in a 100 ml round bottom flask at 50 °C in an oil bath. A white solid separates out immediately. To this 16.51 mmol (4.4 ml) of triphenyl phosphite was added drop wise and temperature was raised slowly up to 70 °C. After half an hour the white solid initially formed redissolved and a clear brown solution was obtained. This brown solution was stirred for next 24 h. This solution was washed with saturated solution of sodium bicarbonate till effervescences ceases, then with water and finally with acetone, resulting in the separation of a white solid which was air dried. Yield (3.210 g; 75 %). Anal. Calc (%) for $C_{30}H_{24}N_6O_2$: C, 72.00; H, 4.8; N, 16.80. Found (%): C, 71.56; H, 4.54; N, 16.81. IR (KBr pellets,cm^{-1}): 3099 (s), 3021 (s), 1623 (vs), 1545 (vs), 1437 (vs), 748 (vs).

Synthesis of probe N^2,$N^{2'}$-bis[(1-ethyl-benzimidazol-2-yl) methyl]biphenyl-2,2'-dicarboxamide ($\mathbf{L_1}$)

To a suspension of (A) (1 mmol) in dry DMF (20 ml), KOH (2 mmol) predissolved in dry DMF (5 ml) was added dropwise and the reaction mixture was stirred at 70 °C for 30 min. Then, ethyl iodide (2.5 mmol) was added drop wise over a time period of 30 min and reaction mixture was further stirred for two hours at 70 °C (Scheme 1). After

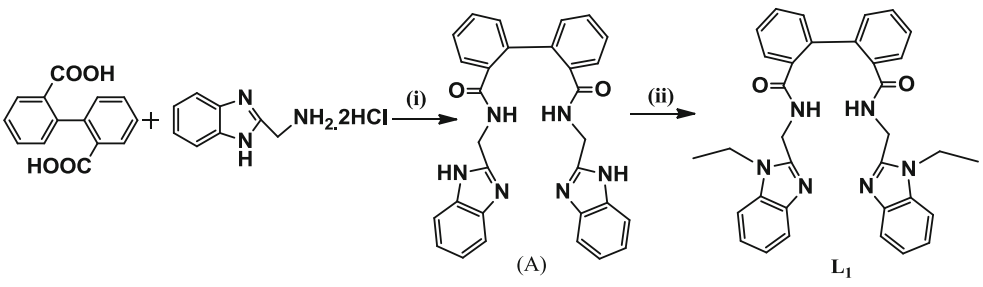

Scheme 1 Reagents and conditions: (*i*) pyridine, triphenyl phosphite; (*ii*) KOH, dry DMF, C_2H_5I

completion of reaction (monitored by TLC), water (50 ml) was added and reaction mixture was extracted with ethyl acetate (3×50 ml). The combined organic layer was dried over Na_2SO_4 and evaporated to get crude compound which was further purified by column chromatography using 2 % methanol in chloroform as eluent. Yield (310 mg; 56 %). Structure of $\mathbf{L}_1$ is confirmed by ^{1}H and ^{13}C NMR spectroscopy, (See supporting information figures S2 and S3), and X-ray diffraction (Fig. 1).

Anal. Calc (%) for $C_{34}H_{32}N_6O_2$: C, 73.36; H, 5.79; N 15.10. Found (%): C, 73.20; H, 5.71; N, 15.17. ^{1}H-NMR (d_6-DMSO, δ_H ppm) 1.16 (t, 6H, 7.2 Hz, CH_3), 4.06 (q, 4H, 7.2 Hz, CH_2), 4.51 (s, 4H, CH_2), 7.05 (dd, 2H, 7.5 & 1.2 Hz), 7.15–7.26 (m, 8H), 7.39 (dd, 2H, 7.6 & 1.4 Hz), 7.45 (dd, 2H, 7.6 & 1.5 Hz), 7.58 (dd, 2H, 7.6 & 1.5 Hz), 9.47 (t, 2H, 5.8 Hz). ^{13}C NMR (d_6-DMSO, δ_C ppm): 14.83, 35.54, 37.82, 110.05, 118.67, 121.44, 122.01, 126.89, 127.04, 128.86, 129.48, 134.63, 135.99, 138.21, 141.92, 150.70, 169.01. IR (KBr pellets, cm^{-1}): 3178 (w), 2978 (w), 2931 (w), 1649 (vs), 1540 (s), 1458 (s), 746 (s). UV–vis (Methanol, λ_{max}, nm, log ε M^{-1}cm^{-1}): 284(4.15), 276(4.17).

Synthesis of the Metallacycle [Cu_3($\mathbf{L}_1$)$_3Cl_3$].3H_2O.3Cl **(1)**

To a methanolic solution of $\mathbf{L}_1$, (0.179 mmol, 5.0 ml), $CuCl_2.2H_2O$ (0.179 mmol), predissolved in 5.0 ml methanol was added dropwise at room temperature. The desired product formed immediately as a green solid. It was filtered, washed with methanol and dried in vacuum over P_2O_5. Yield 80 %. Anal. Calc (%) for $C_{102}H_{96}N_{18}O_6Cl_6Cu_3.3H_2O$: C, 57.58; H, 4.79; N, 11.85. Found (%): C, 57.73; H, 4.82; N, 11.73. IR (KBr pellets, cm^{-1}): 3436 (m) 3199 (m), 3058 (m), 1610 (vs), 1542 (s), 1467 (s), 743 (s). UV–vis (Methanol, λ_{max}, nm, log ε M^{-1} cm^{-1}): 275(4.72), 282(4.66), 740(2.81).

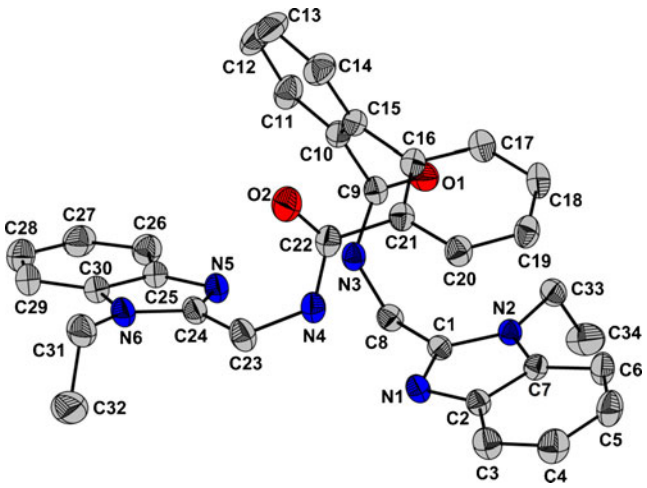

Fig. 1 Ortep diagram of diamide probe $\mathbf{L}_1$ drawn in 30 % thermal probability ellipsoids showing atomic numbering schemes. Hydrogen are omitted for the sake of clarity

Crystal Structure Determination

Single crystals of $\mathbf{L}_1$ & the copper(II) complex **(1)** suitable for X-ray diffraction studies were grown by slow evaporation in ethyl acetate and acetonitrile respectively**.** The intensity data were collected at 298 K on an X'calibur CCD diffractometer with graphite monochromatized Mo/Kα radiation. For $\mathbf{L}_1$, a total of 23225 reflections were measured of which 5683 were unique and 4665 were considered observed ($I>2\sigma(I)$]. For **(1)**, a total of 83382 reflections were measured of which 23043 were unique and 19013 were considered observed ($I>2\sigma(I)$]. The data were corrected for Lorentz and polarization effects. Multi-scan absorption correction was applied. The structure was solved by direct methods using SHELXS-97 [42] and refined by full-matrix least-squares refinement techniques on F^2, using SHELXL-97. All calculations were done with the help of WINGX package of the crystallographic programs [43]. All non-hydrogen atoms were refined anisotropically. All hydrogen atoms were fixed geometrically with Uiso values of 1.2 times the Uiso values of their respective carrier atoms. The final residual index for $\mathbf{L}_1$ are; *R* 0.0490, *R*w 0.1291 for the observed and *R* 0.0624, *R*w 0.1231 for all reflections using 379 parameters. The final residual index for **(1)** are; *R* 0.0604, *R*w 0.1996 for the observed and *R* 0.0724, *R*w 0.2086 for all reflections using 1250 parameters. Thermal ellipsoids plot (ORTEP) for $\mathbf{L}_1$, and **(1)** is shown in Figs. 1 and 8 respectively. Crystal and structure refinement data and selected geometrical parameters are summarized in Tables 1, 2, 3, 4 and 5. CCDC numbers 889023 and 889024.

Results and Discussion

Fluorescence Spectral Studies

The emission spectrum of $\mathbf{L}_1$ was recorded in different solvents. Figure 2 displays the emission spectra of a 100 μM solution of $\mathbf{L}_1$ in CH_3CN, DMF, $CHCl_3$, MeOH and Water (90 %) when excited at 277 nm. In all cases, an emission centered at 300 nm was observed. Since the solubility of $\mathbf{L}_1$ in CH_3CN and water was very poor, a mixture of CH_3CN and $CHCl_3$ (9:1) water and methanol (9:1) was employed. The intensity of the emission at 300 nm (Fig. 2) can be attributed to arise from the Benzimidazolyl moiety [44]. The fluorescence quenching is strongly affected by the nature of the solvent although it does not strictly depend on solvent polarity. Quenching is highest in water and methanol than the other organic solvents like DMF, CH_3CN and chloroform. As PET mediated quenching occurs rapidly in a relatively more polar solvent, the quenching effect cannot be attributed to a PET process in present case [16]. A probable reason for this can be ascribed to the likely H-bonding of water and MeOH hydrogen with the imine N-atom of benzimidazolyl moiety, a

Table 1 Crystal and structure refinement data for $\mathbf{L_1}$ and **(1)**

	$\mathbf{L_1}$	**(1)**
Empirical formula	C34 H32N6 O2	C102 H96 Cl6 Cu3 N18 O9
Formula weight	556.66	2121.29
Temperature	298(2) K	298(2) K
Wavelength	0.71073 Å	0.71073 Å
Crystal system	Monoclinic	Triclinic
Space group	P21/c	$P\bar{1}$
Unit cell dimensions	a=11.5271(5) Å	a=17.4599(6) Å, α=88.659(3)°
	b=9.8804(3) Å, β=95.109(4)°	b=17.5549(6) Å, β=82.865(3)°
	c=25.4924(9) Å 2891.85(18) Å^3	c=22.1720(7) Å, γ=60.573(3)° 5867.7(3) Å^3
Volume	2891.85(18) Å	5867.7(3) Å
Z	4	2
Density (mg/m^3)	1.279	1.201
Absorption coefficient	0.082 mm^{-1}	0.732 mm^{-1}
F(000)	1176	2190
Crystal size	0.22×0.20×0.18 mm^3	0.20×0.14×0.12 mm^3
Θ range for data	3.08 to26.00°	2.86 to 26.00°.
Collection index ranges	$-14\le h\le 13$, $-12\le k\le 12$, $-31\le l\le 31$	$-21\le h\le 21$, $-21\le k\le 21$, $-27\le l\le 27$
Reflections collected	23225	83382
Independent reflections	5683[R(int) = 0.0242]	23043 [R(int) = 0.0358]
Completeness to Θ=26°	99.8 %	99.8 %
Absorption correction	Multi-scan	Multi-scan
Max. and min. transmission	0.9854 & 0.9822	0.9173 and 0.8674
Refinement method	Full-matrix least-squares on F^2	Full-matrix least-squares on F^2
Data/restraints/parameters	5683/0/379	23043/0/1250
Goodness-of-fit on F^2	1.069	1.042
Final R indices [I>2 σ (I)]	$R1$=0.0490, w$R2$=0.1185	$R1$=0.0604, w$R2$=0.1996
R indices (all data)	$R1$=0.0624, w$R2$=0.1240	$R1$=0.0724, w$R2$=0.2086
Largest diff. peak and hole	0.190 and −0.184 e.Å^{-3}	1.412 and −0.522 e.Å^{-3}

situation that does not arise with solvents like CH_3CN, DMF and $CHCl_3$. Wavelength excitation dependence study indicates that there is no significant change in the intensity of both bands (Fig. 3) suggesting that there is no monomer and excimer relationship between the two bands [45].

Table 2 Selected bond lengths (Å) for $\mathbf{L_1}$

Bond	(Å)
C(1)-N(1)	1.316(2)
C(1)-N(2)	1.369(2)
C(8)-N(3)	1.451(2)
C(9)-O(1)	1.231(2)
C(9)-N(3)	1.339(2)
C(15)-C(16)	1.499(2)
C(22)-O(2)	1.218(2)
C(22)-N(4)	1.344(2)
C(23)-N(4)	1.447(2)
C(24)-N(5)	1.314(2)
C(24)-N(6)	1.366(2)

Complexation and Binding

Fluorescence spectral studies were undertaken to decipher the effect of metal ion Complexation on the fluorophore $\mathbf{L_1}$. $\mathbf{L_1}$ (c=100 μM) showed an emission centered at 300 nm due to benzimidazole moiety in MeOH (λ_{ex} 277 nm, quantum yield ϕ_o=0.160) and water methanol mixture (9:1) (λ_{ex}

Table 3 Selected bond lengths (Å) for **(1)**

Bond	(Å)	Bond	(Å)
N(7)-Cu(1)	1.988(3)	O(3)-Cu(2)	2.071(3)
N(5)-Cu(1)	1.974(3)	Cl(2)-Cu(2)	2.2951(10)
O(5)-Cu(1)	2.208(3)	N(1)-Cu(3)	1.995(3)
O(6)-Cu(1)	2.054(2)	N(18)-Cu(3)	1.997(3)
Cl(1)-Cu(1)	2.2762(10)	O(1)-Cu(3)	2.106(3)
N(12)-Cu(2)	1.984(3)	O(2)-Cu(3)	2.207(3)
N(13)-Cu(2)	1.973(3)	Cl(3)-Cu(3)	2.2595(10)
O(4)-Cu(2)	2.209(3)		

Table 4 Selected bond angles (°) for $\mathbf{L_1}$

Bond	angles (°)	Bond	angles (°)
N(1)-C(1)-N(2)	113.47(14)	C(21)-C(16)-C(15)	123.59(14)
N(1)-C(1)-C(8)	122.32(14)	O(2)-C(22)-N(4)	122.76(17)
N(2)-C(1)-C(8)	124.11(14)	O(2)-C(22)-C(21)	122.86(17)
O(1)-C(9)-N(3)	123.29(16)	N(5)-C(24)-N(6)	113.43(16)
O(1)-C(9)-C(10)	121.51(15)	N(5)-C(24)-C(23)	124.11(15)
C(10)-C(15)-C(16)	120.81(14)	N(6)-C(24)-C(23)	122.39(15)

277 nm, quantum yield ϕ_o=0.064). Upon adding increasing amounts of metal ions like Cu^{2+} (12.5–125 μM) as nitrate salt to solution of $\mathbf{L_1}$ the emission at 300 nm was found to be quenched due to the chelation enhanced quenching (CHEQ) effect of metal ions with a slight red shift of the ligand band (Fig. 4). Interestingly a new band around 375 nm (quantum yield ϕ_o=0.146 in methanol and ϕ_o=0.210 in water methanol mixture (9:1)) starts to arise simultaneously upon the addition of metal ions and is attributed to an intraligand π–π* transition within the biphenyl spacer of the ligand [46]. Quantum yields, ϕ were calculated by comparison of the spectra with that of anthracene (ϕ=0.292) taking the area under the total emission. The fluorescence spectra of 20 μM solution (Abs~0.1) in MeOH and H_2O-MeOH mixture (9:1) for $\mathbf{L_1}$ and the isolated copper(II) complex has now been employed for calculation of quantum yields, these have been calculated by utilizing the formula:

$$\phi = \text{area}_{\text{ligand}}/\text{area}_{\text{anth}} \times \text{Abs}_{\text{anth}}/\text{Abs}_{\text{ligand}}$$

where, Abs = absorption of the ligand and anthracene at 277 nm.

Table 5 Selected bond angles (°) for **(1)**

Bond	angles (°)	Bond	angles (°)
N(5)-Cu(1)-N(7)	176.35(12)	O(3)-Cu(2)-O(4)	92.20(11)
N(5)-Cu(1)-O(6)	91.02(11)	N(13)-Cu(2)-Cl(2)	92.28(10)
N(7)-Cu(1)-O(6)	86.11(11)	N(12)-Cu(2)-Cl(2)	92.32(9)
N(5)-Cu(1)-O(5)	87.73(12)	O(3)-Cu(2)-Cl(2)	155.41(9)
N(7)-Cu(1)-O(5)	90.10(11)	O(4)-Cu(2)-Cl(2)	112.30(8)
O(6)-Cu(1)-O(5)	91.81(11)	N(1)-Cu(3)-N(18)	172.99(12)
N(5)-Cu(1)-Cl(1)	91.03(9)	N(1)-Cu(3)-O(1)	89.89(11)
N(7)-Cu(1)-Cl(1)	92.55(9)	N(18)-Cu(3)-O(1)	84.27(12)
O(6)-Cu(1)-Cl(1)	153.48(9)	N(1)-Cu(3)-O(2)	86.55(12)
O(5)-Cu(1)-Cl(1)	114.69(8)	N(18)-Cu(3)-O(2)	89.50(12)
N(13)-Cu(2)-N(12)	175.34(13)	O(1)-Cu(3)-O(2)	89.28(11)
N(13)-Cu(2)-O(3)	90.53(12)	N(1)-Cu(3)-Cl(3)	92.62(9)
N(12)-Cu(2)-O(3)	84.97(12)	N(18)-Cu(3)-Cl(3)	94.27(9)
N(13)-Cu(2)-O(4)	88.25(12)	O(1)-Cu(3)-Cl(3)	157.27(9)
N(12)-Cu(2)-O(4)	90.71(11)	O(2)-Cu(3)-Cl(3)	113.42(9)

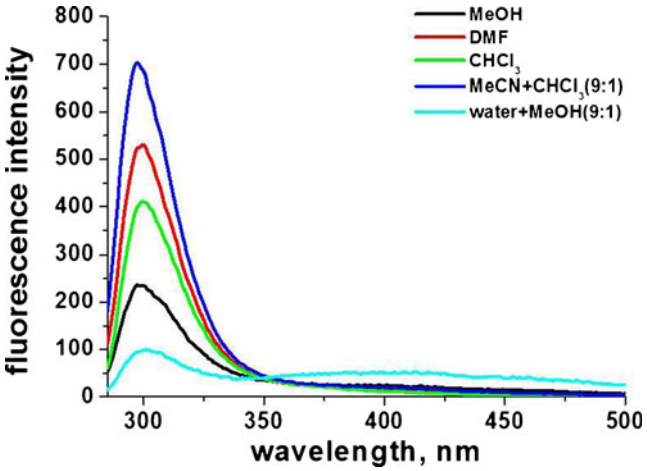

Fig. 2 Emission spectra of diamide $\mathbf{L_1}$ in different solvents (c= 100 μM)

Simultaneous 'quenching' (300 nm band) and the 'enhancement' (375 nm band) is also observed if instead of nitrate salt of copper(II), chloride salt of copper(II) is utilized for the titration experiment. This confirms a minimal role of co-anion chloride or nitrate in the 'quenching' and 'enhancement' behavior and confirms that the change is brought about by the metal ion. (See supporting information, figure S4). This behavior is again found for isolated Cu(II) complex **(1)** with $\mathbf{L_1}$ where only 375 nm band is observed while the 300 nm band is quenched (See supporting information, figure S5). This 'enhancement' of the 375 nm band could be ascribed to chelation enhanced fluorescence (CHEF), that causes increased rigidity of the biphenyl ring, reducing the non radiative decay of the intraligand excited state [47–49]. The above fact is supported by a decrease in the dihedral angle between the plane of two phenyl rings, being 76.03(6)° in ligand $\mathbf{L_1}$ and dropping to 48.79(16)° upon complexation with Cu^{+2} confirming greater rigidity in the copper bound ligand. No such behavior was

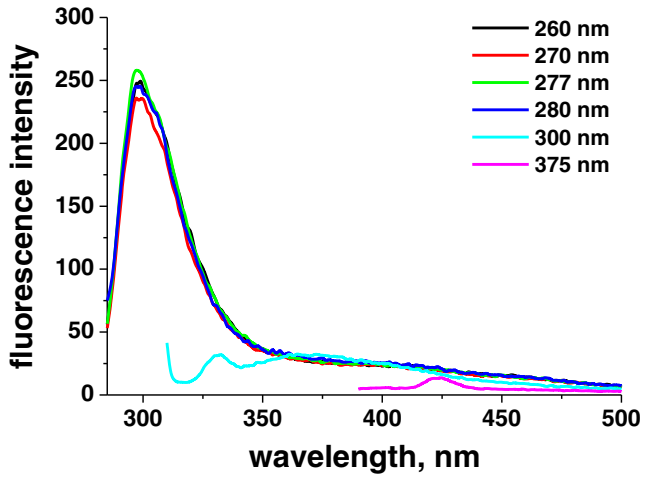

Fig. 3 Emission spectra of diamides $\mathbf{L_1}$ after excitation at different wavelengths in MeOH (c=100 μM)

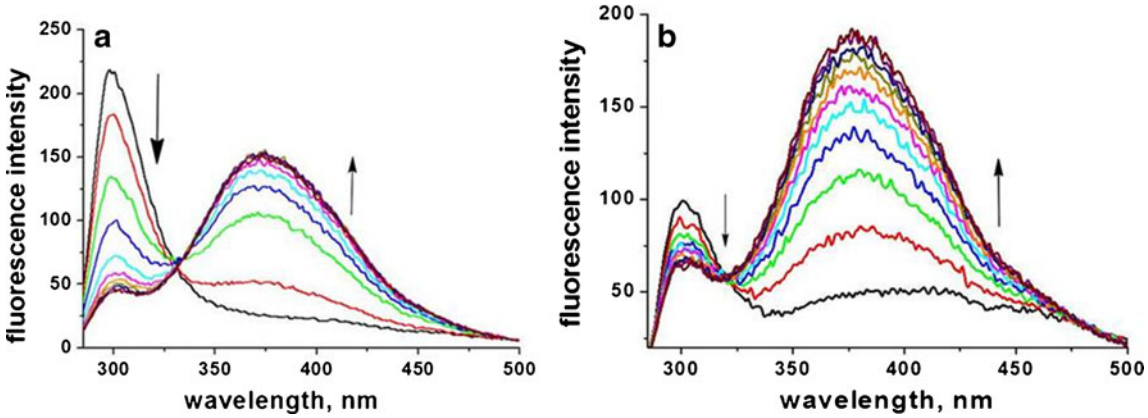

Fig. 4 **a:** Fluorescence titration of $\mathbf{L_1}$ (c=100 μM) with Cu^{2+} in methanol and **b:** water–methanol mixture (9:1) with increasing Cu^{2+} concentration (12.5–125 μM)

observed in case of other metal ions even when a large excess of metal ion (5 equiv.) were added, except for Zn^{2+} in methanol and Pb^{2+} in aqueous solution (90 % H_2O) where a slight increase (10 % and 25 % respectively) in the 375 nm band is observed. (See supporting information, figures S6(a)–S6(g) & S7(a)–S7(g)).

The binding constant (log K 4.69 M^{-1} & 4.72 M^{-1} in MeOH and water methanol mixture (9:1) respectively) of $\mathbf{L_1}$

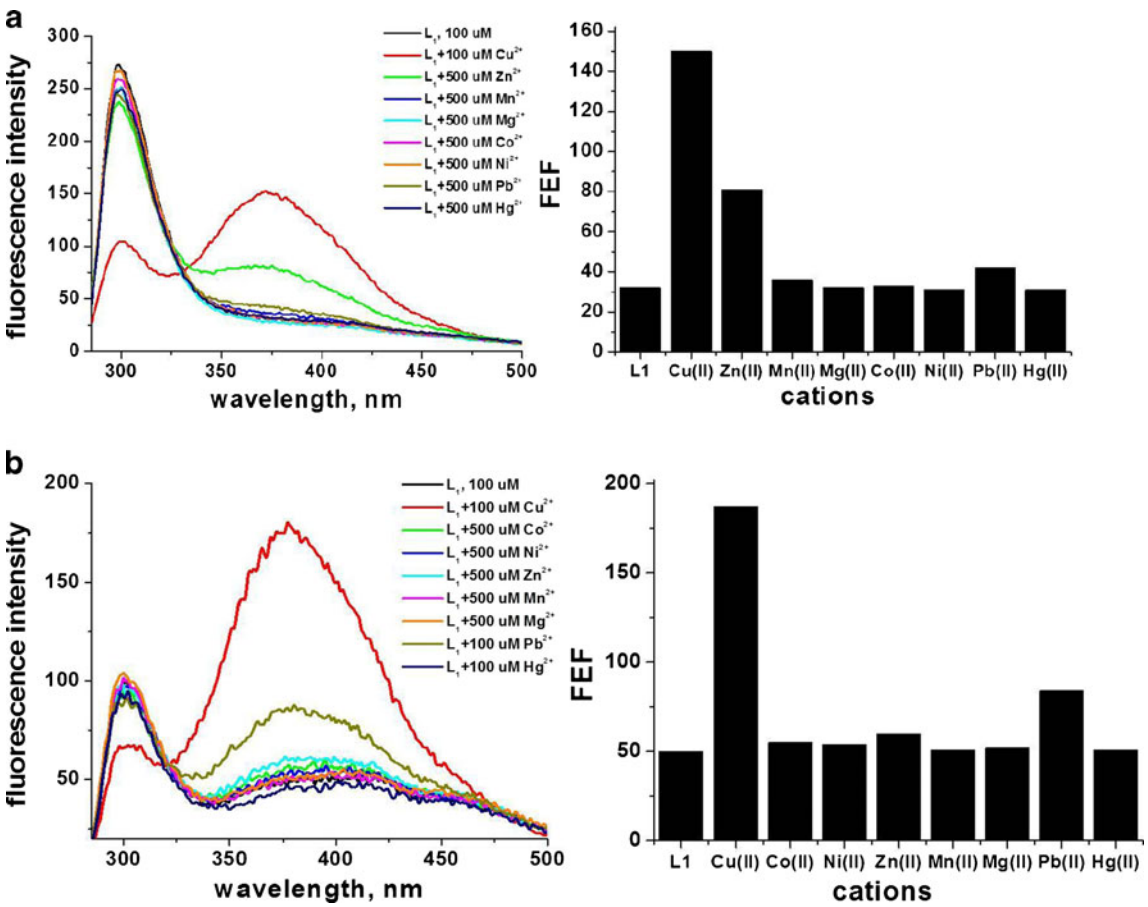

Fig. 5 **a:** Emission response of $\mathbf{L_1}$ (c=100 μM) upon addition of Cu^{2+} (1 equivalent) and other metal ions (5 equivalents,) in Methanol (*left*) and fluorescence enhancement factor (FEF) upon addition of Cu^{2+} (1 equivalent) and other metal ions (5 equivalents) (*right*). Excitation and emission wavelength at 277 nm and 375 nm, respectively. **b:** Emission response of $\mathbf{L_1}$ (c=100 μM) upon addition of Cu^{2+} (1 equivalent) and other metal ions (5 equivalents,) in water–methanol mixture (9:1) (*left*) and fluorescence enhancement factor (FEF) upon addition of Cu^{2+} (1 equivalent) and other metal ions (5 equivalents) (*right*). Excitation and emission wavelength at 277 nm and 375 nm, respectively

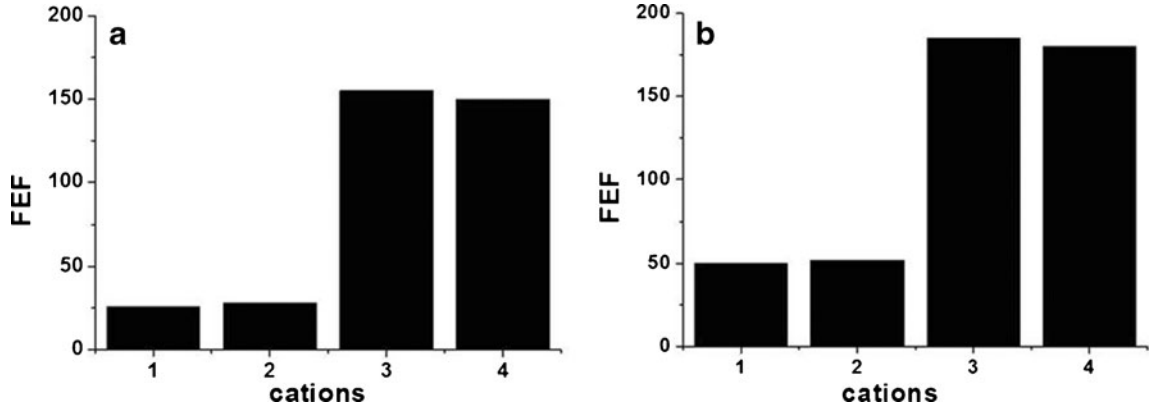

Fig. 6 **a:** Fluorescence enhancement factor (in methanol) of $\mathbf{L_1}$ (*c*= 100 μM, *column 1*); $\mathbf{L_1}$ (*c*=100 μM, in presece of other metal ions, (5 equivalents) except Cu^{2+} & Zn^{2+}, *column 2*); $\mathbf{L_1}$ (*c*=100 μM, and Cu^{2+}, 1 equivalent, *column 3*); $\mathbf{L_1}$ (*c*=100 μM, upon addition of Cu^{2+}, (1 equivalent) in presence of other metal ions (5 equivalent) except Zn^{2+}, *column 4*). Excitation and emission wavelength at 277 nm and 375 nm, respectively. **b:** Fluorescence enhancement factor (in water–methanol mixture (9:1)) of $\mathbf{L_1}$ (*c*=100 μM, *column 1*); $\mathbf{L_1}$ (*c*= 100 μM, in presece of other metal ions, (5 equivalents) except Cu^{2+} & Pb^{2+}, *column 2*); $\mathbf{L_1}$ (*c*=100 μM, and Cu^{2+}, 1 equivalent, *column 3*); $\mathbf{L_1}$ (*c*=100 μM, upon addition of Cu^{2+}, (1 equivalent) in presence of other metal ions (5 equivalent) except Pb^{2+}, *column 4*). Excitation and emission wavelength at 277 nm and 375 nm, respectively

with Cu(II) was calculated by the Benesi-Hildebrand equation [50–52]. The measured intensity [1/(*F*−*F*0)] at 375 nm varied as a function of 1/[Cu^{2+}] in a linear relationship (See supporting information figure S8). The binding constant is found to be smaller than those reported with other ligating system [10, 53].

Selectivity Studies

To investigate the selective preference of $\mathbf{L_1}$, metal ions such as Cu^{2+}, Ni^{2+}, Co^{2+}, Mn^{2+}, Mg^{2+}, Zn^{2+}, Pb^{2+} and Hg^{2+} were added to the solution of $\mathbf{L_1}$ in MeOH and water–methanol mixture (9:1). Upon addition of Cu^{2+} (108 μM) in methanol and water methanol mixture (9:1) to $\mathbf{L_1}$ (100 μM), the fluorescence intensity at 375 nm is significantly enhanced (from 25 intensity units to 150 units, six fold enhancement and from 50 intensity units to 185 units, approximately. Four fold enhancement, respectively) (Fig. 5a & b). However, upon the addition of other metal ions, the fluorescence enhancement was lower than 50 fold (Fig. 5a and b). Therefore $\mathbf{L_1}$ has preference only for Cu^{2+}. A competition experiment was also investigated by adding Cu^{2+} (100 μM) to the solution of $\mathbf{L_1}$ (100 μM) in the presence of other metal ions (500 μM) Fig. 6a and b shows that the presence of other metal ions did not interfere in the detection of Cu^{2+} even if they are present in fivefold excess except Zn^{2+} in methanol and except Pb^{2+} in Water–methanol mixture (9:1) which have a mild interference. Although Fe^{3+} has a significant interference.

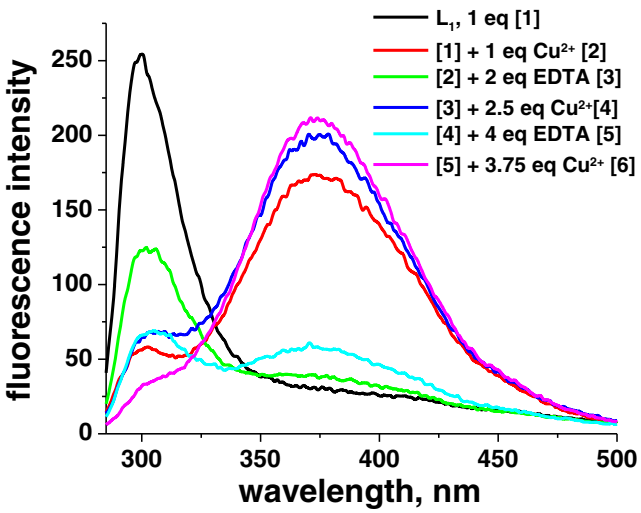

Fig. 7 Signaling "off-on-off" behaviour of $\mathbf{L_1}$ upon alternate addition of Cu^{2+} and Na_2EDTA to $\mathbf{L_1}$ (*c*=100 μM) in methanol

Off-On-Off Switch

Several molecular machines have been developed that have a recognition system based on a lock and key mechanism [27, 54]. It was therefore of interest to find if the present system possesses such a recognition system or not. The system does work like a molecular 'Lock' which requires a 'Key' copper(II) to open it (generation of 375 nm band) and Na2-EDTA to lock the system back (loss of 375 nm band). Diamide ligand $\mathbf{L_1}$ under investigation exhibits reversible fluorescence enhancement (turn-on)/quenching (turn-off) in the presence of Cu^{2+}/Na_2-EDTA, respectively. The fluorescent intensity of 375 nm bands in $\mathbf{L_1}$ enhances (turns-on) upon addition of Cu^{2+} and quenches (turn-off) upon addition of Na_2-EDTA, cycling at least three times (Fig. 7). As Na_2-EDTA is a much better chelating agent than the present fluorophore $\mathbf{L_1}$, hence it chelates Cu^{2+} more strongly and releases the ligand $\mathbf{L_1}$, thus the band at 375 nm is 'turned off' upon addition of Na_2-EDTA.

Electronic Absorption Studies

The electronic absorption spectrum of $\mathbf{L_1}$ show two sharp peaks in the UV region at 276 and 284 nm arising due to π–π* transition in benzimidazolyl moiety [55]. These peaks are slightly shifted and appear at 271–280 nm upon addition of Cu^{2+} ions, while the shoulder around 249 nm disappears. The blue shift in the position of absorption bands in comparison to $\mathbf{L_1}$ may be attributed to the formation of a complex. (See supporting information, figure S9 and S10). While other metal ions displayed insignificant changes. A similar blue shift in the UV region was also observed for the isolated copper(II) complex (20 μM) in methanol and water–methanol mixture (See supporting information, figure S11).

IR Spectral Studies

The free ligands $\mathbf{L_1}$ have characteristic IR bands at 1649 cm^{-1}, assigned to amide I ($\nu_{C=O}$). The band at 1540 cm^{-1} is assigned to amide II ($\nu_{C\text{-}N}$), while the band at 1458 cm^{-1} is assigned to $\nu_{C=N\text{-}C=N}$ stretching of the benzimidazole group. These bands are shifted by 30–40 cm^{-1} in the complex, thus, implying a direct coordination of the imine nitrogen and amide carbonyl to the metal site [56].

Crystal Structure Description

The ORTEP diagram of $\mathbf{L_1}$ and **(1)** with atomic numbering scheme is shown in Figs. 1 and 8 respectively. The diamide ligand $\mathbf{L_1}$ crystallizes in monoclinic P21/c space group with one molecule in asymmetric unit. The dihedral angle between the planes of two phenyl rings in biphenyl was found to be 76.03(6)°. The single crystal of copper(II) complex with ligands $\mathbf{L_1}$ with co-anion chloride was found to be suitable for single crystal diffraction work. Complex **(1)** crystallizes in triclinic P-1 space group. The crystals were air sensitive and the data was collected in paraton oil. The complex is a metallatriangle with three copper atoms lying at the vertices of a scalene triangle with three ligands (average Cu-Cu distance 10.437 Å). Each copper(II) ion is five coordinate with a highly distorted square pyramidal geometry (Fig. 8). The geometry is best described as a distorted square pyramidal with Addison parameters τ=0.38 for Cu1, τ=0.33 for Cu2 and τ= 0.26 for Cu3. The parameter τ is defined as $\tau = (\alpha–\beta)/60$, ($\alpha > \beta$), where α and β are the largest angles; α=1 for a regular trigonal bipyramid and τ=0 for a regular square pyramid [57]. The basal plane of the square pyramid is formed by two nitrogen atoms (N5 & N7 for Cu1, N12 & N13 for Cu2 and N1 & N18 for Cu3) and two oxygen atoms (O5 & O6 for Cu1, O3 & O4 for Cu2 and O1 & O2 for Cu3) of the benzimidazolyl diamide ligand and the apical position of the Cu(II) is occupied by the Cl1, Cl2 and Cl3 anion respectively (Fig. 8) Three chlorides are present in lattice to balance the charge. The average dihedral angle between the planes of two phenyl rings in biphenyl is found to be 48.79(16)°. Complex **(1)** shows an A level alert containing solvent accessible voids in the unit cell. These voids were calculated by SOLV routine of PLATON [58] and showing voids of 1108.1 $Å^3$. Unit cell also contains three water molecules in the lattice out of which two are found to be disordered over two positions in 60:40 ratios.

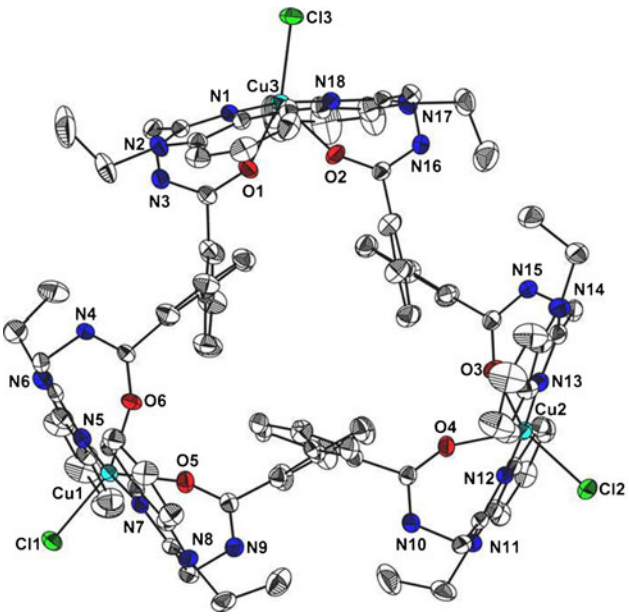

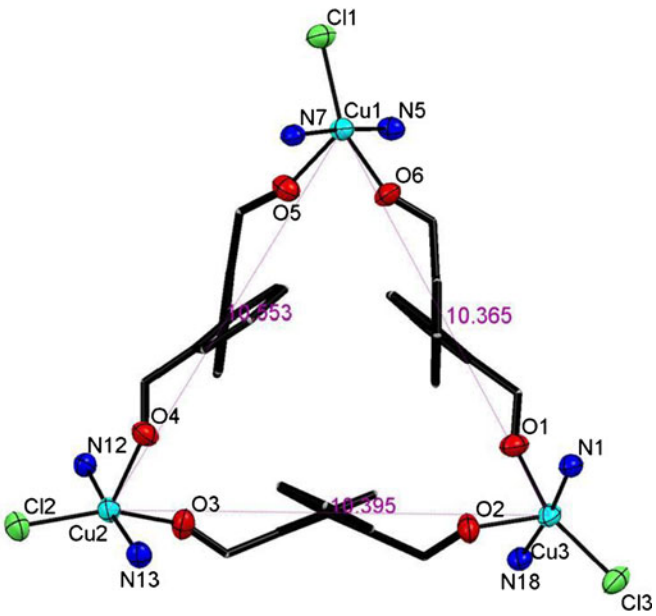

Fig. 8 Ortep diagram of cation $[Cu_3(\mathbf{L_1})_3Cl_3]^{3+}$ of **(1)** drawn in 30 % thermal probability ellipsoids showing partial atomic numbering schemes. Hydrogen, lattice anions and solvent water are omitted for the sake of clarity (*left*) and Ortep diagram showing distorted square pyramidal geometry around the copper(II) in **(1)**. Benzimidazole moiety have been omitted for a better visulization of the geometry around Cu(II) ion (*right*)

Conclusions

In summary, we have described the synthesis, elemental and spectral characterization of *bis*-benzimidazolyl diamide ligand $\mathbf{L_1}$ and its copper(II) trinuclear metallacycle. The structure of diamide $\mathbf{L_1}$ and its Cu(II) metallacycle complex **(1)** was further confirmed by X-ray single crystallography. The diamide $\mathbf{L_1}$ shows a simultaneous 'quenching' (300 nm band) and 'enhancement' (375 nm band) in the presence of Cu^{2+}. $\mathbf{L_1}$ selectively detects Cu^{2+} in the presence of other metal ions like Mn^{2+}, Mg^{2+}, Ni^{2+}, Co^{2+}, and Zn^{2+}. The diamide $\mathbf{L_1}$ shows "off-on-off" signaling behavior towards Cu^{2+} in the presence of Na_2-EDTA.

Acknowledgments The authors are grateful to University of Delhi, Delhi for a special grant. We are thankful to USIC-CIF, University of Delhi, Delhi, India for NMR and Single Crystal X-ray data. One of the authors is thankful to UGC for providing senior research fellowship (SRF).

References

1. Lovstad RA (2004) A kinetic study on the distribution of Cu(II)-ions between albumin and transferrin. BioMetals 17:111–113
2. Que EL, Domaille DW, Chang CJ (2008) Metals in neurobiology: probing their chemistry and biology with molecular imaging. Chem Rev 108:1517–1549
3. Gaggelli E, Kozlowski H, Valensin D, Valensin G (2006) Copper homeostasis and neurodegenerative disorders (Alzheimer's, Prion, and Parkinson's Diseases and Amyotrophic Lateral Sclerosis). Chem Rev 106:1995–2044
4. Jung HS, Park M, Han DY, Kim E, Lee C, Ham S, Kim JS (2009) Cu2+ ion-induced self-assembly of pyrenylquinoline with a pyrenyl excimer formation. Org Lett 11:3378–3381
5. Zheng Y, Gattas-Asfura KM, Konka V, Leblanc RM (2002) A dansylated peptide for the selective detection of copper ions. Chem Commun 2350–2351
6. Jung et al (2009) Coumarin-derived Cu^{2+} -selective fluorescence sensor: synthesis, mechanisms, and applications in living cells. J Am Chem Soc 131:2008–2012
7. Weng YQ, Yue F, Zhong YR, Ye BH (2007) A Copper(II) ion-selective on-off-type fluoroionophore based on zinc porphyrin–dipyridylamino. Inorg Chem 46:7749–7755
8. Xu Z, Yoon J, Spring DR (2010) Fluorescence chemosensors for Zn^{2+}. Chem Soc Rev 39:1996–2006
9. Callan JF, De Silva AP, Magri DC (2005) Luminescent sensors and switches in the early 21st century. Tetrahedron 61:8551–8588
10. Li J et al (2011) A novel rhodamine-benzimidazole conjugate as a highly selective turn-on fluorescent probe for Fe^{3+}. J Fluoresc 21:2005–2013
11. Khatua S, Choi SH, Lee J, Huh JO, Do Y, Churchill DJ (2009) Highly selective fluorescence detection of Cu^{2+} in water by chiral dimeric Zn^{2+} complexes through direct displacement. Inorg Chem 48:1799–1801
12. Royzen M, Dai Z, Canary JW (2005) Ratometric displacement approach to Cu(II) sensing by fluorescence. J Am Chem Soc 127:1612–1613
13. Wolf C, Mei XF, Rokadia HK (2004) Selective detection of Fe(III) ions in aqueous solution with a 1,8-diacridylnaphthalene-derived fluorosensor. Tetrahedron Lett 45:7867–7871
14. Ballesteros E et al (2009) A new selective chromogenic and turn-on fluorogenic probe for copper(II) in water–acetonitrile 1:1 solution. Org Lett 11:1269–1272
15. Shin DH, Ko YG, Choi US, Kim WN (2006) Bowing effect with fluorescence: a unique chemosensor for the silver ion. Ind Eng Chem Res 45:656–662
16. Formica M, Fusi V, Giorgi L, Micheloni M (2012) New fluorescent chemosensors for metal ions in solution. Coord Chem Rev 256:170–192
17. De Silva SA, Zavaleta AD, Baron E (1997) A fluorescent photo-induced electron transfer sensor for cations with an off-on-off proton switch. Tetrahedron Lett 38:2237–2240
18. De Silva SA et al (2005) A fluorescent "off-on-off" proton switch derived from natural products and further studies of first-generation fluorescent photoinduced electron transfer (PET) systems. J Mater Chem 15:2791–2795
19. De Silva SA et al (2002) A fluorescent "off-on-off" proton switch with an overriding 'enable-disable' sodium ion switch. Chem Commun 1360–1361
20. Callan JF, De Silva AP, McClenaghanb ND (2004) Switching between molecular switch types by module rearrangement: Ca^{2+}-enabled, H^+-driven 'off-on-off', H^+-driven YES and PASS 0 as well as H^+, Ca^{2+}-driven AND logic operations. Chem Commun 2048–2049
21. Goswami P, Das DK (2011) Significant effect of surfactant micelles on pH dependent fluorescent off-on-off behavior of Salicylaldehyde-2,4-Dinitrophenylhydrazone. J Luminescence 131:760–763
22. Bandyopadhyay P, Ghosh AK (2009) pH controlled "off-on-off" switch based on Cu^{2+}-mediated pyrene fluorescence in a PAA–SDS micelle aggregated supramolecular system. J Phys Chem B 113:13462–13464
23. Pais VF et al (2011) Off-on-off fluorescence switch with T-Latch function. Org Lett 13:5572–5575
24. Fabbrizzi L, Gatti F, Pallavicini P, Parodi L (1998) An "off-on-off" fluorescent sensor for pH based on ligand–proton and ligand–metal–proton interactions. New J Chem 1403–1407
25. Zhang HG et al (2011) Off-on-off luminescent switching of a dye containing imidazo[4, 5-f][1, 10]phenanthroline. Chin Chem Lett 22:647–650
26. Ravikumar I, Ghosh P (2011) Zn(II) and PPi selective fluorescence off-on-off functionality of a chemosensor in physiological conditions. Inorg Chem 50:4229–4231
27. Pandey R et al (2011) Fluorescent zinc(II) complex exhibiting "on-off-on" switching toward Cu^{2+} and Ag^+ ions. Inorg Chem 50:3189–3197
28. Barceloux DG, Barceloux D (1999) Copper. J Toxicol Clin Toxicol 37:217–230
29. Zhang XB, Peng J, He CL, Shen GL, Yu RQ (2006) A highly selective fluorescent sensor for Cu^{2+} based on 2-(2′-hydroxyphenyl)benzoxazole in a poly(vinyl chloride) matrix. Anal Chim Acta 567:189–195
30. Sarkar B (1981) In Metal ions in biological systems. Siegel H, Siegel A (eds.) Marcel Dekker, New York 12:233
31. Georgopoulos PG, Roy A, Yonone-Lioy MJ, Opiekun RE, Lioy PJ (2001) Environmental copper: its dynamics and human exposure issues. J Toxicol Environ Health B 4:341–394
32. Tak WT, Yoon SC (2001) Clinical significance of blood level of zinc and copper in chronic renal failure patients. KSN 20:863–871
33. Zheng Y et al (2003) Development of fluorescent film sensors for the detection of divalent copper. J Am Chem Soc 125:2680–2686
34. Zheng Y et al (2001) A new fluorescent chemosensor for copper ions based on tripeptide Glycyl–Histidyl–Lysine (GHK). Org Lett 3:3277–3280
35. Zheng Y et al (2003) Design of a membrane fluorescent sensor based on photo-cross-linked PEG hydrogel. J Phys Chem B 107:483–488

36. Goswami S, Chakrabarty R (2009) Fluorescence sensing of Cu2+ within a pseudo 18-crown-6 cavity. Tetrahedron Lett 50:5910–5913
37. Liu Z, Yang Z, Li T, Wang B, Li Y, Qin D, Wang M, Yan M (2011) An effective Cu(II) quenching fluorescence sensor in aqueous solution and 1D chain coordination polymer framework. Dalton Trans 40:9370–9373
38. Costero AM, Gil S, Sanchis J, Peransi S, Sanz V, Williams JAG (2004) Conformationally regulated fluorescent sensors. Study of the selectivity in Zn^{2+} versus Cd^{2+} sensing. Tetrahedron 60:6327–6334
39. Cescon LA, Day AR (1962) Preparation of some benzimidazolylamino acids. Reactions of amino acids with o-phenylenediamines. J Org Chem 27:581–586
40. Mahiya K, Mathur P (2013) Morphology dependent oxidation of aromatic alcohols by new symmetrical copper (II) metallatriangles formed by self-assembly of a shared bis -benzimidazolyl diamide ligand. Inorganica chimica Acta. doi:10.1016/j.ica.2012.12.037
41. Barnes DJ, Chapman RL, Vagg RS, Watton EC (1978) Synthesis of novel bis(amides) by means of triphenyl phosphite intermediates. J Chem Eng Data 23:349–350
42. Sheldrick GM (1997) SHELXS97 and SHELXL97; program for crystal structure solution and refinement. University of Gottingen, Germany
43. Farrugia LJ (1999) WinGX suite for small-molecule single-crystal crystallography. J Appl Crystallogr 32:837–838
44. Kumar A, Sinha HK, Dogra SK (1989) Electronic spectrum of bibenzimidazole homologue: effects of solvents and acid concentration. Can J Chem 67:1200–1205
45. Huang HW et al (1996) Fluorescence study on intermolecular interactions between mesogenic biphenyl moieties of a thermotropic liquid-crystalline polyester (PB-10). Macromolecules 29:3485–3490
46. Guo F, Xu J, Zhang X, Zhu B (2010) Hydrothermal synthesis, crystal structures and photoluminescent properties of four cadmium(II) coordination polymers derived from diphenic acid and auxiliary ligands. Inorg Chim Acta 363:3790–3797
47. Zhang LY et al (2003) Helical ribbons of Cadmium(II) and Zinc(II) dicarboxylates with bipyridyl-like chelates–syntheses, crystal structures and photoluminescence. Eur J Inorg Chem 2003:2965–2971
48. Chen W et al (2003) Photoluminescent metal–organic polymer constructed from trimetallic clusters and mixed carboxylates. Inorg Chem 42:944–946
49. Yam VWW, Lo KKW (1999) Luminescent polynuclear d10 metal complexes. Chem Soc Rev 28:323–334
50. Benesi HA, Hildebrand JH (1949) A spectrophotometric investigation of the interaction of iodine with aromatic hydrocarbons. J Am Chem Soc 71:2703–2707
51. Barra M, Bohne C, Scaiano JC (1990) Effect of cyclodextrin complexation on the photochemistry of xanthone. Absolute measurement of the kinetics for triplet-state exit. J Am Chem Soc 112:8075–8079
52. Xie G et al. (2012) A highly selective fluorescent and colorimetric chemosensor for ZnII and its application in cell imaging. Eur J Inorg Chem 327
53. Ghosh K, Sen T, Patra A (2010) Binding induced destruction of an excimer in anthracene-linked benzimidazole diamide: a case toward the selective detection of organic sulfonic acids and metal ions. New J Chem 34:1387–1393
54. Huo F-J, Su Y-Q, Su J, Yang Y-T, Yin C-X, Chao J-B (2010) Chromene “lock”, thiol “key”, and Mercury(II) ion “hand”: a single molecular machine recognition system. Org Lett 12:4756–4759
55. Monzani E et al (1998) Tyrosinase models. synthesis, structure, catechol oxidase activity, and phenol monooxygenase activity of a dinuclear copper complex derived from a triamino pentabenzimidazole ligand. Inorg Chem 37:553–562
56. Tehlan S, Hundal MS, Mathur P (2004) Copper(II) complexes of N-Octylated Bis(benzimidazole) diamide ligands and their peroxide-dependent oxidation of aryl alcohols. Inorg Chem 43:6589–6595
57. Addison AW, Rao TN, Reedijk J, Rijn JV, Verschoor GC (1984) Synthesis, structure, and spectroscopic properties of Copper(II) compounds containing nitrogen-sulphur donor ligands; the crystal and molecular structure of Aqua[l,7-bis(N-methylbenzimidazol-2′-yl)-2,6-dithiaheptane]copper(II) Perchlorate. J Chem Soc Dalton Trans 1349–1356
58. Spek AL (2003) Single-crystal structure validation with the program. PLATON J Appl Crystallogr 36:7–13